Finite Element Model Updating for Tension-Stabilized Flexible Space Structures

Finite Element Model Updating for Tension-Stabilized Flexible Space Structures

Hiraku SAKAMOTO[1)], Yuuki OKADA[1)], and Nozomu KOGISO[2)]

[1)] *Tokyo Institute of Technology, Tokyo, Japan*
[2)] *Osaka Prefecture University, Osaka, Japan*

Structural parameters in a geometrically nonlinear finite-element (FE) model are updated so that the experimental measurements are precisely reproduced by the FE model. In addition, the confidence intervals of the estimated parameters are obtained by a bootstrap method. This study evaluates the applicability of the analysis methods by carrying out a simple experiment. The experimental model consists of a flexible beam and cable, which are in an equilibrium of internal forces under finite deformation. This experimental model simulates a future space reflector.

Key Words: FEM, bootstrap, reliability, confidence interval, parameter estimation

1. Introduction

Recent space structures, especially for reflector applications, tend to become larger and more precise than conventional space structures. For example, Japan Aerospace Exploration Agency is developing the radio astronomy satellite, Astro-G, whose reflector is approximately 10m in diameter, and has a 0.4mmRMS surface accuracy. The reflector of Astro-G consists of flexible ribs, cables, and meshes. After the reflector's deployment, the ribs are elastically deformed by the tensions in the cables to form a curved surface.

It is challenging to test such flexible structures on the ground due to gravity. Since tests using full-scale hardware is often not feasible, tests have to be compensated by a high-fidelity numerical model. Finite element (FE) methods are commonly used. Tension-stabilized structures like Astro-G's reflector require geometrically nonlinear analysis, in which the finite deformation of flexible ribs and the geometric stiffness due to the introduction of internal forces are taken into account. In addition, attachment of actuators on the ribs has been discussed for shape control. For example, piezo-electric actuators for space use have been developed[1].

When numerical models of space structures are fitted to experimentally measured data, it is required to consider uncertainties in the experimental measurements. In other words, when parameters in the numerical models are determined, how much the parameter values possibly distribute has to be also quantified. The confidence intervals (CI) with a particular confidence level are often used to quantify the reliability of a parameter estimation.

From these backgrounds, the present study applies the following methods to a simple experimental model that simulates flexible rib and cable structures, aiming at evaluating the applicability of the following methods:

- Parameters in a geometrically nonlinear FE model are updated so that the experimental measurements are reproduced precisely by the FE model.
- Deformations caused by piezo-electric actuators are also precisely modeled by the FE method.
- Uncertainties in the estimated FE parameters due to the uncertainties in experimental measurements are evaluated by obtaining confidence intervals. The bootstrap method[2,3] is used.

This paper is organized as follows. Section 2 explains the experimental model that is used the evaluation of the analysis methods. Section 3 describes the analysis methods being evaluated. Section 4 shows the results and discussions.

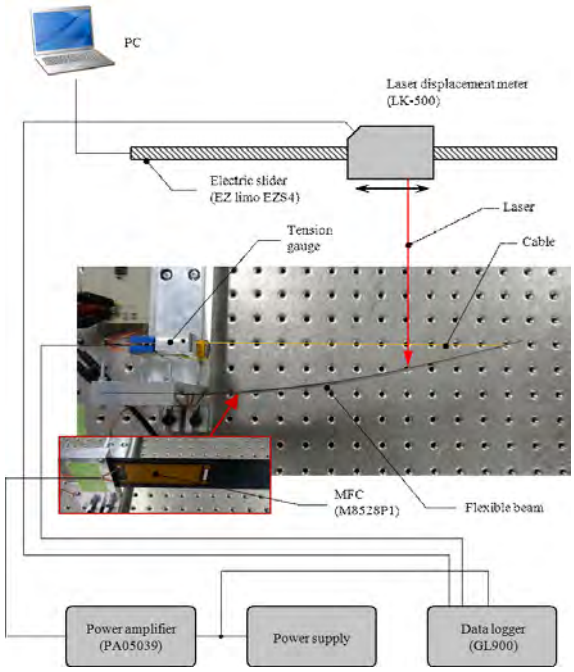

Fig. 1 Experimental setup.

2. Experimental model of tension-stabilized structure

Figure 1 shows the experimental setup. The flexible beam is made of spring steel, with 250mm in length, 50mm in width, and 0.5mm in thickness. The beam is initially straight in its undeformed configuration. A steal cable applies a tension to the beam and the structures are in equilibrium. The tension level exerted in the cable is approximately 4 N. A macro-fiber composite (MFC) actuator is attached at the beam's root. Figure 2 shows the MFC actuator itself. At the root of the cable, a tension gauge is attached to measure the tension in the cable for verification of the analysis.

The deformed beam shape is measured by a laser displacement sensor attached on a linear slider. Since the FE model computes

Fig. 2 Macro-fiber composite (MFC) actuator.[1]

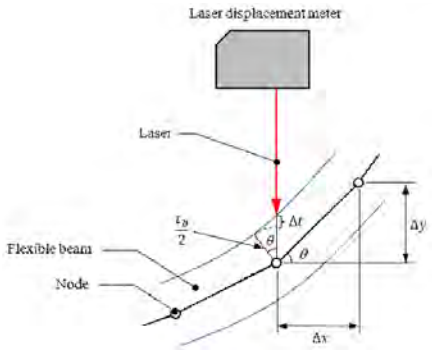

Fig. 3 Consideration of thickness of beam.

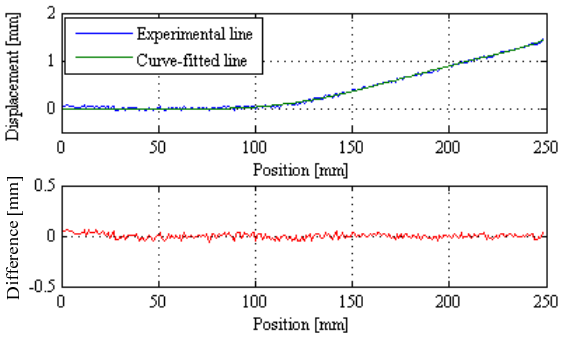

Fig. 4 One of measured beam shapes and curve fitting result.

the deformation of the center line of the beam, the experimental measurement data are processed to the displacement at the center line by the consideration of the beam thickness, as depicted in Fig. 3. The laser displacement sensor measures the displacement every 1mm along the beam length. In addition, the measured shape is smoothed out, after eliminating some outliers, using a polynomial fitting as shown in Fig. 4.

3. Analysis methods

This section describes the FE model of the experimental model, the FE updating method, and the bootstrap method that provides the CIs of the estimated parameters.

3·1 Construction of FE model Figure 5(a) illustrates an early FE model constructed by the authors. The commercial FE package ABAQUS is used. The flexible beam is represented by 2D Euler-Bernoulli beam elements. The cable is represented by 2D truss elements. Finally, the MFC actuator is represented by piezo-electric elements, and they are connected to the beam elements using geometrical constraints.

In the early model, as shown in Fig. 5(a), boundary conditions at beam's and cable's roots were fixed ones. However, with this boundary conditions, the FE model could not precisely fit to

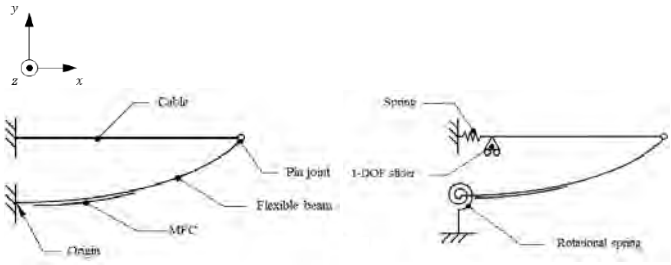

(a) Preliminary model (b) Refined model

Fig. 5 Boundary conditions of finite-element (FE) models.

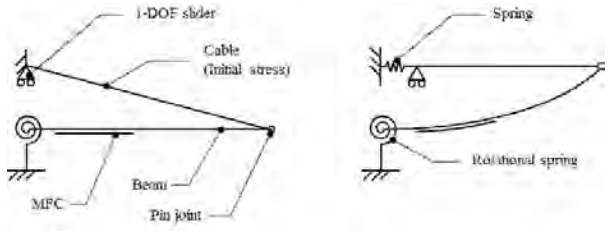

(a) Initial shape (b) Deformed shape

Fig. 6 Procedure of FE computation in geometrically nonlinear analysis.

experimental results. Therefore, the FE model was updated to the one illustrated in Fig. 5(b). The rotational spring at beam's root, with the spring constant K_{rb}, represents the effect of non-ideal cantilever clamping. The translational spring at cable's root represents the flexibility of the tension gauge. This new model realizes much close fitting of the FE model to the experimental results.

Figure 6 shows the procedure of the FE computation in the geometrically nonlinear FE analysis framework. In the initial step of the analysis, the initial configuration depicted in Fig. 6(a) is used. In this configuration, the cable is pre-stressed with the pre-stress of P_c. Then the equilibrium configuration, depicted in Fig. 6(b), is computed iteratively by the Newton-Raphson method.

3·2 FE updating method The beam's deformed shape is very sensitive to some parameters in the FE model. In addition, some parameters in the FE model are unable to measure precisely in separate experiments. Therefore, these parameters are updated so that the FE prediction of deformed shape approaches to the experimental result. The FE updating algorithm used in this study is as follows.

First, let $x_1, \cdots, x_n$ are the FE parameters that are subject to updating, and $y_1, \cdots, y_m$ are the displacements at m measurement points.

$$\mathbf{x} = [x_1,\ x_2,\ \cdots,\ x_n]^T \tag{1}$$

$$\mathbf{y}(\mathbf{x}) = [y_1(\mathbf{x}),\ y_2(\mathbf{x}),\ \cdots,\ y_m(\mathbf{x})]^T \tag{2}$$

At the k-th iteration, let $\mathbf{x} = \mathbf{x}_k$. In addition, let $\mathbf{x}_E$ is the set of ideal parameters that coincides the FE result and the experimental measurement. By Taylor expansion,

$$\mathbf{y}(\mathbf{x}_E) \approx \mathbf{y}(\mathbf{x}_k) + \left[\frac{\partial \mathbf{y}(\mathbf{x})}{\partial \mathbf{x}}\right]_{\mathbf{x}=\mathbf{x}_k} \Delta\mathbf{x}_k \tag{3}$$

where $k = 0, 1, \cdots$. Then the parameter updating law is given by $\mathbf{x}_{k+1} = \mathbf{x}_k + \Delta\mathbf{x}_k$ where

$$\Delta\mathbf{x}_k = \left[\frac{\partial \mathbf{y}(\mathbf{x})}{\partial \mathbf{x}}\right]^{+}_{\mathbf{x}=\mathbf{x}_k} \{\mathbf{y}(\mathbf{x}_E) - \mathbf{y}(\mathbf{x}_k)\} \tag{4}$$

In Eq. (4), $[\ \ ]^+$ means a pseudo-inverse. The above procedure is repeated until all the components of $|\mathbf{y}(\mathbf{x}_E)-\mathbf{y}(\mathbf{x}_k)|$ becomes smaller than a threshold.

In Eqs. (3·2) and (4), the sensitivities, $\left[\frac{\partial \mathbf{y}(\mathbf{x})}{\partial x_i}\right]_{x_i=x_{ik}}$ where $i=1,\cdots,n$, are the deformation mode with respect to the updating parameters, In this study, these values are computed by partial differences using ABAQUS analysis. these sensitivities are calculated in each iteration.

In this study, the following parameters are updated: the rotational spring constant at the beam root, K_{rb}, the Young's modulus of the MFC actuator, E_M, and the initial stress introduced in the cable, P_c.

3·3 Bootstrap method Finally, the confidence intervals of the estimated FE parameters are obtained by bootstrap methods[2,3].

Step 1: Carry out the experimental shape measurements N times to obtain $\mathbf{y}_1,\ \mathbf{y}_2,\ \cdots,\mathbf{y}_N$.

Step 2: From the data $\mathbf{y}_1,\ \mathbf{y}_2,\ \cdots,\mathbf{y}_N$, randomly extract N samples, $\mathbf{Y}_1,\ \mathbf{Y}_2,\ \cdots,\mathbf{Y}_N$, allowing repetition (**resampling**). Calculate the average shape from the resampled data as:

$$\bar{\mathbf{Y}}=\frac{1}{N}\sum_{i=1}^{N}\mathbf{Y}_i \tag{5}$$

Then estimate the FE model parameters, $(\hat{K}_{rb},\hat{E}_M,\hat{P}_c)$, that minimizes $||\bar{\mathbf{Y}}-\hat{\mathbf{y}}(\hat{K}_{rb},\hat{E}_M,\hat{P}_c)||$ where $\hat{\mathbf{y}}$ is the beam shape predicted by the FE analysis.

Step 3: Repeat Step 2 for B times. As a result, B estimations are obtained such as $\hat{K}_{rb}^{(1)},\ \hat{K}_{rb}^{(2)},\ \cdots,\hat{K}_{rb}^{(B)}$. ($\hat{E}_M^{(j)}$ and $\hat{P}_c^{(j)}$ are similarly obtained where $j=1,\cdots,B$.) Note that $\hat{K}_{rb}^{(j)}$, $\hat{E}_M^{(j)}$ and $\hat{P}_c^{(j)}$ herein are sorted in ascending order respectively.

Step 4: When the required confidence level is $1-\alpha$, the confidence interval (CI) for $\hat{K}_{rb}$ is given as follows (**Percentile bootstrap CI**[2]).

$$\left[\hat{K}_{rb}^{\left(\frac{\alpha}{2}B\right)},\quad \hat{K}_{rb}^{\left(\left(1-\frac{\alpha}{2}\right)B\right)}\right] \tag{6}$$

And CIs for $\hat{E}_M$ and $\hat{P}_c$ are similarly given.

4. Results and discussion

4·1 Results of FE updating Figure 7 shows the comparison between one of the experimentally measured shape and the FE result calculated using a initial set of parameters. The initial parameters are determined by catalog value (E_M) and guessing (K_{rb} and P_c). The deformed shape of the beam is not precisely predicted; the overall error is 0.740 mmRMS.

The three parameters in the FE model, (K_{rb},E_M,P_c), are updated by the FE updating algorithm described in §3.2. In this study, $n=3$ and $m=251$. Figure 8 shows the difference between the experimental result and the FE prediction after the convergence of the algorithm. The residual is 0.017 mmRMS. Figure 9 shows the results when the MFC actuator is driven by the voltages of 200V and 400V respectively. The FE analysis results correlate the experimental results quite accurately.

4·2 Estimation of confidence interval (CI) The results of confidence interval calculation described in §3.3 especially change when the number of experiments changes. In this study, the three cases, $N=5,10,20$, are compared where N is the number of experiments. In fact, the experiments were carried out 30 times. Five different sets of experimental data are extracted in each case

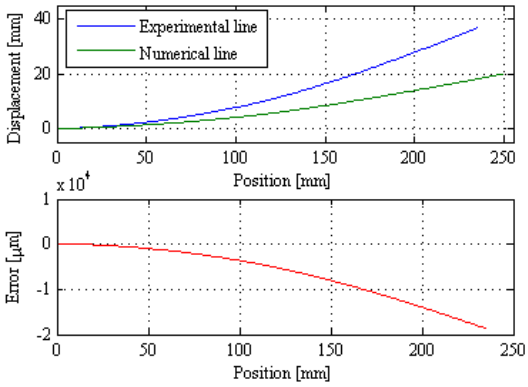

Fig. 7 Experimental result and initial FE model's result.

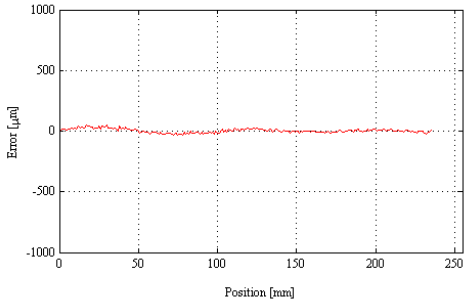

Fig. 8 Difference between experiment and FE analysis after FE-model updating.

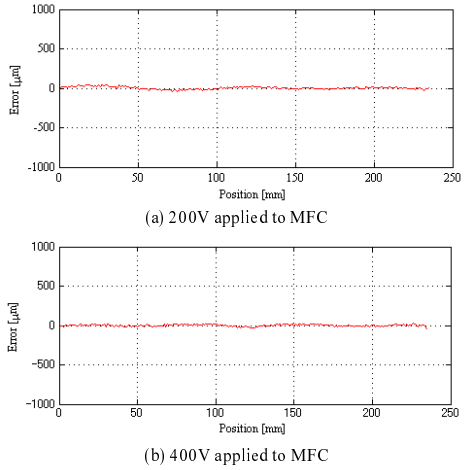

Fig. 9 Difference between experiment and FE analysis after FE-model updating with MFC actuation.

of $N=5,10,20$ respectively to observe the distribution of CIs. In every case, the number of bootstrap resampling, B, is 100, and the confidence level is set at $1-\alpha=95\%$.

Figure 10 shows the CIs of the rotational spring constant at the beem root, K_{rb}, obtained by bootstrap method. The blue histograms show the distribution of the estimated parameter, the two blue lines show the lower and upper bounds of the CIs for the particular cases. Finally, the two red lines show the lowest lower bounds and highest upper bounds of the CIs for five cases. Table 1 and 2 show the same results by numbers. Two things can be observed. First, the CI is significantly wider when $N=5$ than the other two cases. In

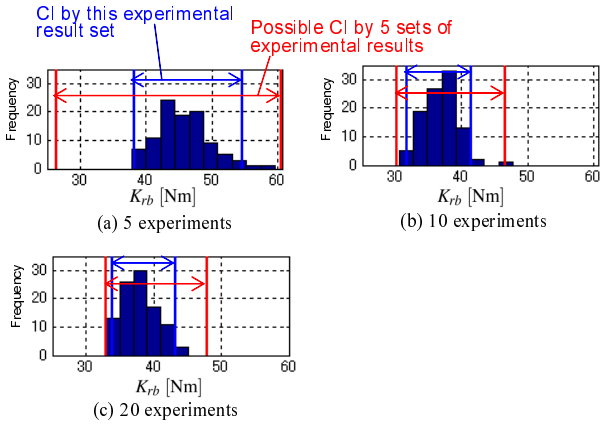

Fig. 10 Distribution and 95% confidence interval (CI) of estimated rotational spring constant.

Table 1 95% confidence intervals (CI) of rotational spring constant estimated by bootstrap method using one set of experimental results.

Number of experiments	*CI* [Nm]	*Interval width* [Nm]
5	$[3.828 \times 10^1, \quad 5.461 \times 10^1]$	1.633×10^1
10	$[3.184 \times 10^1, \quad 4.152 \times 10^1]$	9.682×10^0
20	$[3.380 \times 10^1, \quad 4.318 \times 10^1]$	9.380×10^0

Table 2 Lowest lower bound and highest upper bound of 95% CI of rotational spring constant estimated by bootstrap method using five sets of experimental results.

Number of experiments	*CI* [Nm]	*Interval width* [Nm]
5	$[2.637 \times 10^1, \quad 6.054 \times 10^1]$	3.417×10^1
10	$[3.028 \times 10^1, \quad 4.667 \times 10^1]$	1.639×10^1
20	$[3.288 \times 10^1, \quad 4.797 \times 10^1]$	1.509×10^1

other words, the FE parameters estimated by only five experiments are less reliable. Second, the CIs of $N = 10$ and $N = 20$ cases are not substantially different. This result may imply that 10 experiments are enough for this system and significant improvement in parameter estimation cannot be expected even if more number of experiments are carried out. Further investigations will clarify this issue.

Acknowledgements

H. Sakamoto is supported by Japan Society for the Promotion of Science (JSPS), Grant-in-Aid for Young Scientists (B).

References

(1) Wilkie, W. K., Inman, D. J., Lloyd, J. M., and High, J. W., "Anisotropic Piezocomposite Actuator Incorporating Machined PMN-PT Single Crystal Fibers," AIAA Paper 2004–1889, 2004.

(2) Wang, J., Taguri, M., Tezuka, S., Kabashima, Y., and Ueda, N., *Computational Statistics I*, Iwanami Publishers, 2003, (in Japanese).

(3) Konishi, S., Ochi, M., and Omori, Y., *Methods in Computational Statistics, –Bootstrap, EM algorithm, MCMC–*, Asakura Publishing, 2008, (in Japanese).